Available online at www.sciencedirect.com
ScienceDirect
International Journal of Solids and Structures 44 (2007) 5043–5055
INTERNATIONAL JOURNAL OF SOLIDS and STRUCTURES
www.elsevier.com/locate/ijsolstr

Softening hyperelasticity for modeling material failure: Analysis of cavitation in hydrostatic tension

K.Y. Volokh

Faculty of Civil and Environmental Engineering, Technion–Israel Institute of Technology, Haifa 32000, Israel

Received 13 March 2006; received in revised form 15 December 2006
Available online 22 December 2006

Abstract

Material failure analysis based on the constitutive model of isotropic softening hyperelasticity is presented. In addition to the bulk and shear moduli the model includes only one material constant of volumetric failure work. The latter is in contrast to the traditional damage theories, which include internal variables that are difficult to calibrate experimentally. The softening hyperelasticity model is used to analyze the critical hydrostatic tension corresponding to the onset of instability of spherical and cylindrical voids. It is shown that the critical tension predicted by the softening hyperelasticity model does not depend on the void size in agreement with the linear elasticity solution showing that the stress/strain state at the edge of the void does not depend on its size. This prediction stays in contrast to the prediction based on the Griffith energy method where the critical tension depends on the size of the void and tends to infinity when the void radius approaches zero. It is argued that the controversial results of the Griffith method are a consequence of a separation of stress analysis and criticality conditions. It is concluded, based on the considered examples, that a description of material failure should be an inseparable part of constitutive models of materials.

Keywords: Void; Hyperelasticity; Softening; Failure; Damage

1. Introduction

The basic idea underlying bulk failure modeling is to introduce a damage parameter, scalar or tensor, which describes the degradation of material properties during mechanical loading: Kachanov (1958, 1986), and Krajcinovic (1996), Skrzypek and Ganczarski (1999), Lemaitre and Desmorat (2005). The damage parameter is an internal variable though its possible interpretation as a volumetric density of voids or microcracks is reasonable. The magnitude of the damage parameter is constrained by (a) a damage evolution equation and (b) a critical threshold condition similar to the plasticity theories. Potentially, the approach of damage mechanics is very flexible and allows reflecting the physical processes triggering macroscopic damage at small length scales. Practically, the experimental calibration of damage theories is far from trivial. It is difficult to measure the damage parameter directly. The experimental calibration should be implicit and it should include both the

E-mail address: cvolokh@tx.technion.ac.il

0020-7683/$ - see front matter
doi:10.1016/j.ijsolstr.2006.12.022

damage evolution equation and the damage criticality condition. Because of these difficulties, it seems reasonable to look for alternative theories that present the bulk material failure in more feasible ways than the traditional damage theories. Softening hyperelasticity is a possible candidate for a simple description of material failure.

The roots of the softening hyperelasticity approach can be traced to atomistic analysis of fracture relating material debonding to atomic separation. Gao and Klein (1998) and Klein and Gao (1998) (and, more recently, Volokh and Gao, 2005) showed how to mix the atomistic and continuum material descriptions in order to simulate the fracture process. They applied the Cauchy–Born rule linking microscopic and macroscopic length scales to empirical potentials, which include a possibility of the full atomic separation. The continuum–atomistic linkage called the Virtual Internal Bond method led to the formulation of macroscopic strain energy potentials allowing for the stress/strain softening and strain localization. The VIB method is very effective at small length scales where purely atomistic analysis becomes computationally intensive. This approach found applications in bio- and nano-mechanics concerning the problems of bone fracture (Gao et al., 2003; Ji and Gao, 2004) and strength of carbon nanotubes (Zhang et al., 2004; Volokh and Ramesh, 2006). Unfortunately, the direct use of the ideas of Gao and Klein in macroscopic damage problems is not very feasible because the computer implementation of the VIB method includes a numerically involved procedure of the averaging of the interatomic potentials over a representative volume.

As a macroscopic alternative to the VIB method a phenomenological softening hyperelasticity approach for modeling material failure has been announced by Volokh (2004) and it is developed and applied to the problems of cavitation in the present study. The basic idea of the phenomenological softening hyperelasticity approach is to formulate (find) an expression of the strain-energy, which enforces stress/strain softening. An example of such strain-energy potential is discussed below. It is crucial that the presented material model is characterized by two standard constants—shear and bulk moduli—and only one additional constant of the *volumetric failure work*, which can be readily calibrated in experiments. The proposed softening hyperelasticity model of material failure is applied to the problems of spherical and cylindrical void expansion under hydrostatic tension. It is shown that the critical tension corresponding to the instability of the void and initiation of the dynamic failure propagation does not depend on the size of the void. The latter is in harmony with the results of linear elasticity that predict independence of stresses and strains at the void edge on the void size. The observation of the void-size-independent critical tension obtained by using the softening hyperelasticity approach is remarkably different from the critical tension prediction based on the Griffith (1921) energy approach widely adapted in the classical fracture mechanics: Bazant and Planas (1998), Broberg (1999), Hertzberg (1989), Kanninen and Popelaar (1973), and Knott (1985). We postpone the discussion of this interesting issue to the last section of the present work.

The paper is organized as follows. We formulate the softening hyperelasticity concept in Section 2.1. Then, we show how to solve the problem of spherical and cylindrical voids under a hydrostatic tension in Sections 2.2 and 2.3 accordingly. The results of the solution are presented in Section 2.4. After that, we analyze the cavitation problem by using the Griffith energy method in Sections 3.1 and 3.2 for spherical and cylindrical voids accordingly. A discussion of the obtained results and comparison of the softening hyperelasticity and Griffith approaches is given in the last section of the work.

2. Softening hyperelasticity

2.1. Governing equations

We set the strain energy per unit volume in the form

$$W = \Phi - \Phi\left(1 + \sqrt{K/\Phi}\ \mathrm{tr}\,\boldsymbol{\varepsilon}\right)\exp\left(-\sqrt{K/\Phi}\ \mathrm{tr}\,\boldsymbol{\varepsilon} - (\mu/\Phi)\mathbf{e}:\mathbf{e}\right), \tag{2.1}$$

where $\mathbf{e} = \boldsymbol{\varepsilon} - (\mathrm{tr}\,\boldsymbol{\varepsilon})\mathbf{1}/3$ is the deviatoric strain; coefficients K and μ are the bulk and shear moduli, respectively; and Φ is a new constant of the isotropic brittle solid—volumetric failure work. Its dimension is work per unit volume, i.e. it is the same as the dimension of K and μ and the dimension of stress. It is worth emphasizing that the introduced volumetric failure work is different from the separation work traditionally used in the cohesive-

surface-approach to fracture (or the energy release rate of the classical fracture mechanics), which dimension is work per unit area. In the subsequent analysis, we assume that $\boldsymbol{\varepsilon}$ is a tensor of small strains.

The physical meaning of the proposed strain energy expression can be clarified by using a schematic diagram shown in Fig. 1. If the material deformation is different from pure hydrostatic compression then the strain energy approaches a limit value Φ as a function of an equivalent strain measure $|\boldsymbol{\varepsilon}|$. Such energy limit shows that the material cannot sustain arbitrarily large deformations. This is in contrast to the convex energy function of linear elasticity or polyconvex energy functions of other hyperelastic material models that allow for arbitrarily large deformation without failure.

Stresses defined by the softening hyperelasticity model (2.1) take the form

$$\boldsymbol{\sigma} = \frac{\partial W}{\partial \boldsymbol{\varepsilon}} = 2\tilde{\mu}\boldsymbol{\varepsilon} + (\tilde{K} - 2\tilde{\mu}/3)(\operatorname{tr}\boldsymbol{\varepsilon})\mathbf{1}, \tag{2.2}$$

where

$$\tilde{\mu} = \mu\left(1 + \sqrt{K/\Phi}\,\operatorname{tr}\boldsymbol{\varepsilon}\right)\exp\left(-\sqrt{K/\Phi}\,\operatorname{tr}\boldsymbol{\varepsilon} - (\mu/\Phi)\mathbf{e}:\mathbf{e}\right), \tag{2.3}$$

and

$$\tilde{K} = K\exp\left(-\sqrt{K/\Phi}\,\operatorname{tr}\boldsymbol{\varepsilon} - (\mu/\Phi)\mathbf{e}:\mathbf{e}\right) \tag{2.4}$$

are the nonlinear shear and bulk moduli, which depend on strains.

The motivation for the specific choice of the strain energy function comes from the consideration of simple shear and hydrostatic pressure.

In the case of simple shear

$$\tau = \sigma_{12} = \sigma_{21}, \quad \gamma = \varepsilon_{12} = \varepsilon_{21}, \tag{2.5}$$

(2.2) reduces to

$$\frac{\tau}{\Phi} = 2\frac{\mu}{\Phi}\gamma\exp\left(-2\frac{\mu}{\Phi}\gamma^2\right). \tag{2.6}$$

The shape of this curve appears in Fig. 2a. Qualitatively, this means that the magnitude of the shear stress increases with the shear strain, reaches a maximum, and then approaches zero with increasing separation. The local maximum of the curve is at point $\gamma_{\max} = \pm\sqrt{\Phi/4\mu}$. Assume, for example, that the maximum shear for the given material is

$$\gamma_{\max} = 10^{-3}. \tag{2.7}$$

Then we have

$$\mu/\Phi = 2.5 \times 10^5. \tag{2.8}$$

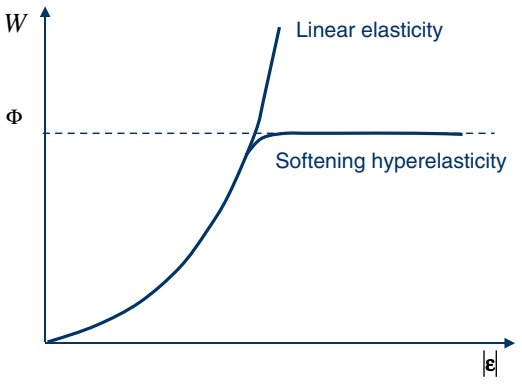

Fig. 1. Linear elasticity without limiters of the strain energy versus softening hyperelasticity with a limited magnitude of the strain energy.

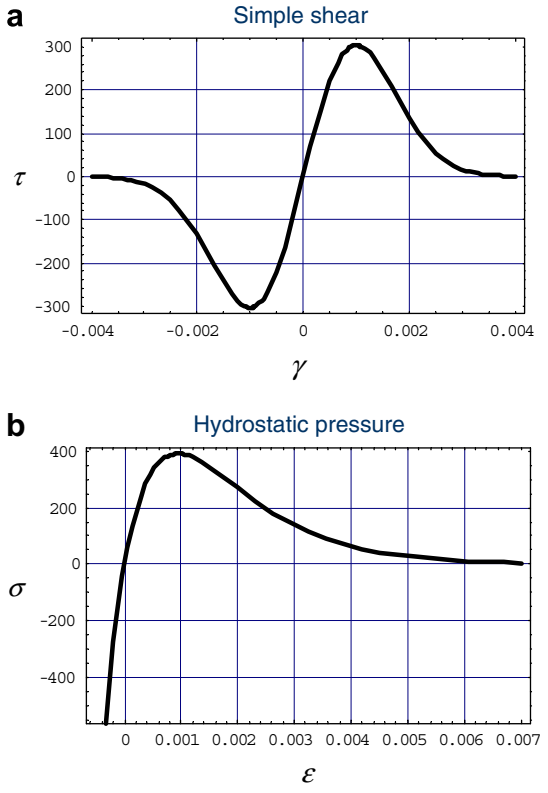

Fig. 2. Physical motivation of the softening hyperelasticity model with simple shear (a) and hydrostatic pressure (b).

Substituting (2.8) in (2.6) we obtain

$$\frac{\tau}{\Phi} = 5 \times 10^5 \gamma \exp\left(-5 \times 10^5 \gamma^2\right). \tag{2.9}$$

The graph of this function is shown in Fig. 2a. In the case of pure hydrostatic pressure

$$\boldsymbol{\sigma} = \sigma \mathbf{1}, \quad \boldsymbol{\varepsilon} = \varepsilon \mathbf{1}, \tag{2.10}$$

(2.2) reduces to

$$\frac{\sigma}{\Phi} = 3\frac{K}{\Phi}\varepsilon \exp\left(-3\sqrt{\frac{K}{\Phi}}\varepsilon\right). \tag{2.11}$$

The shape of this curve appears in Fig. 2b. Qualitatively, it can be interpreted as increase of tension with the increase of the material volume at the point, it reaches a maximum, and then approaches zero with increasing separation. The latter is nothing but the void nucleation.

Assume that material is defined by $K/\mu = 1.5$, for example, then

$$K/\Phi = 3.75 \times 10^5 \tag{2.12}$$

and (2.11) takes the form

$$\frac{\sigma}{\Phi} = 11.25 \times 10^5 \varepsilon \exp\left(-\sqrt{11.25 \times 10^5}\varepsilon\right). \tag{2.13}$$

The graph of this function is shown in Fig. 2b.

Equilibrium equations and natural boundary conditions for the softening hyperelasticity model defined by (2.1) are obtained by varying the total energy with respect to displacements

$$\delta E_{\text{total}} = \delta \int_{\Omega} W \, \mathrm{d}V - \int_{\partial\Omega} \bar{\mathbf{t}} \cdot \delta \mathbf{u} \, \mathrm{d}A, \tag{2.14}$$

where Ω is a body under consideration with boundary $\partial\Omega$ where tractions $\bar{\mathbf{t}}$ or displacements $\mathbf{u}$ are prescribed. In case of small strains, we have the following local equilibrium equations and boundary conditions accordingly

$$\operatorname{div}\boldsymbol{\sigma} = \mathbf{0}, \tag{2.15}$$

$$\boldsymbol{\sigma}\mathbf{n} = \bar{\mathbf{t}}, \tag{2.16}$$

where $\mathbf{n}$ is a unit outward normal.

Finally, we should note that linearizing Eq. (2.2) with respect to strains we obtain the classical equations of linear elasticity

$$\boldsymbol{\sigma} = 2\mu\boldsymbol{\varepsilon} + (K - 2\mu/3)(\operatorname{tr}\boldsymbol{\varepsilon})\mathbf{1}. \tag{2.17}$$

This same result is obtained alternatively by setting $\Phi \to \infty$ in (2.3) and (2.4) in correspondence with Fig. 1.

2.2. Spherical void

Let us consider centrally symmetric deformation of a spherical void—Fig. 3 (left). In this case displacements and strains take the following form in spherical coordinates $\{r,\theta,\varphi\}$:

$$\mathbf{u} = u(r)\mathbf{k}_r, \tag{2.18}$$

$$\boldsymbol{\varepsilon} = \tfrac{1}{2}\left(\nabla\mathbf{u} + \nabla\mathbf{u}^{\mathrm{T}}\right) = \varepsilon_{rr}\mathbf{k}_r \otimes \mathbf{k}_r + \varepsilon_{\theta\theta}\mathbf{k}_\theta \otimes \mathbf{k}_\theta + \varepsilon_{\varphi\varphi}\mathbf{k}_\varphi \otimes \mathbf{k}_\varphi, \tag{2.19}$$

$$\varepsilon_{rr} = \frac{\partial u}{\partial r}; \quad \varepsilon_{\theta\theta} = \frac{u}{r}; \quad \varepsilon_{\varphi\varphi} = \frac{u}{r}, \tag{2.20}$$

where

$$\begin{cases} \mathbf{k}_r = (\sin\theta\cos\varphi,\ \sin\theta\sin\varphi,\ \cos\theta)^{\mathrm{T}}, \\ \mathbf{k}_\theta = (\cos\theta\cos\varphi,\ \cos\theta\sin\varphi,\ -\sin\theta)^{\mathrm{T}}, \\ \mathbf{k}_\varphi = (-\sin\varphi,\ \cos\varphi,\ 0)^{\mathrm{T}}. \end{cases} \tag{2.21}$$

In this case, the stress tensor takes the following form

$$\boldsymbol{\sigma} = \sigma_{rr}\mathbf{k}_r \otimes \mathbf{k}_r + \sigma_{\theta\theta}\mathbf{k}_\theta \otimes \mathbf{k}_\theta + \sigma_{\varphi\varphi}\mathbf{k}_\varphi \otimes \mathbf{k}_\varphi, \tag{2.22}$$

$$\begin{cases} \sigma_{rr} = 2\tilde{\mu}\varepsilon_{rr} + (\tilde{K} - 2\tilde{\mu}/3)\operatorname{tr}\boldsymbol{\varepsilon}, \\ \sigma_{\theta\theta} = 2\tilde{\mu}\varepsilon_{\theta\theta} + (\tilde{K} - 2\tilde{\mu}/3)\operatorname{tr}\boldsymbol{\varepsilon}, \quad , \\ \sigma_{\varphi\varphi} = 2\tilde{\mu}\varepsilon_{\varphi\varphi} + (\tilde{K} - 2\tilde{\mu}/3)\operatorname{tr}\boldsymbol{\varepsilon}. \end{cases} \tag{2.23}$$

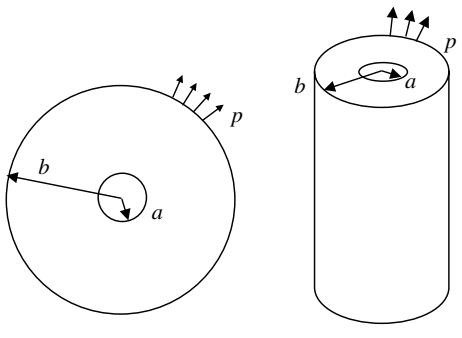

Fig. 3. Spherical and cylindrical cavities under hydrostatic tension.

and equilibrium Eq. (2.15) reduces to

$$\frac{\partial \sigma_{rr}}{\partial r} + 2\frac{\sigma_{rr} - \sigma_{\theta\theta}}{r} = 0. \tag{2.24}$$

Two boundary conditions are imposed on it

$$\begin{cases} \sigma_{rr}(r = a) = 0, \\ \sigma_{rr}(r = b) = p. \end{cases} \tag{2.25}$$

Substituting (2.20) and (2.23) in (2.24) and (2.25), we obtain a nonlinear two-point boundary value problem in terms of radial displacement u.

2.3. Cylindrical void

Let us consider axially symmetric and plane strain deformation of a cylindrical void—Fig. 3 (right). In this case, displacements and strains take the following form in cylindrical coordinates $\{r, \theta, z\}$:

$$\mathbf{u} = u(r)\mathbf{k}_r, \tag{2.26}$$

$$\boldsymbol{\varepsilon} = \tfrac{1}{2}\left(\nabla\mathbf{u} + \nabla\mathbf{u}^{\mathrm{T}}\right) = \varepsilon_{rr}\mathbf{k}_r \otimes \mathbf{k}_r + \varepsilon_{\theta\theta}\mathbf{k}_\theta \otimes \mathbf{k}_\theta, \tag{2.27}$$

$$\varepsilon_{rr} = \frac{\partial u}{\partial r}; \quad \varepsilon_{\theta\theta} = \frac{u}{r}, \tag{2.28}$$

where

$$\begin{cases} \mathbf{k}_r = (\cos\theta, \sin\theta, 0)^{\mathrm{T}} \\ \mathbf{k}_\theta = (-\sin\theta, \cos\theta, 0)^{\mathrm{T}} \\ \mathbf{k}_z = (0, 0, 1)^{\mathrm{T}} \end{cases}. \tag{2.29}$$

In this case, the stress tensor takes the following form

$$\boldsymbol{\sigma} = \sigma_{rr}\mathbf{k}_r \otimes \mathbf{k}_r + \sigma_{\theta\theta}\mathbf{k}_\theta \otimes \mathbf{k}_\theta + \sigma_{zz}\mathbf{k}_z \otimes \mathbf{k}_z, \tag{2.30}$$

$$\begin{cases} \sigma_{rr} = 2\tilde{\mu}\varepsilon_{rr} + (\tilde{K} - 2\tilde{\mu}/3)\,\mathrm{tr}\,\boldsymbol{\varepsilon} \\ \sigma_{\theta\theta} = 2\tilde{\mu}\varepsilon_{\theta\theta} + (\tilde{K} - 2\tilde{\mu}/3)\,\mathrm{tr}\,\boldsymbol{\varepsilon}, \\ \sigma_{zz} = (\tilde{K} - 2\tilde{\mu}/3)\,\mathrm{tr}\,\boldsymbol{\varepsilon} \end{cases} \tag{2.31}$$

and equilibrium Eq. (2.15) reduces to

$$\frac{\partial \sigma_{rr}}{\partial r} + \frac{\sigma_{rr} - \sigma_{\theta\theta}}{r} = 0. \tag{2.32}$$

Two boundary conditions are imposed on it

$$\begin{cases} \sigma_{rr}(r = a) = 0, \\ \sigma_{rr}(r = b) = p. \end{cases} \tag{2.33}$$

Substituting (2.28) and (2.31) in (2.32) and (2.33) we obtain a nonlinear two-point boundary value problem in terms of the radial displacement u.

2.4. Results

Numerical solution of the described problems is generated by using the shooting method with a displacement control. According to it, we, first, make the initial guess for displacement $u^{(0)}$ at the void surface $r = a$. Second, we calculate $(\partial u/\partial r)^{(0)}$ at the void surface from condition $(2.25)_1$ or $(2.33)_1$. Third, we solve the initial value problem with given $u^{(0)}$ and $(\partial u/\partial r)^{(0)}$. The latter step is accomplished by using the 'NDSolve' numerical integrator of Mathematica for the solution of the initial value problem. Three mentioned steps are repeated

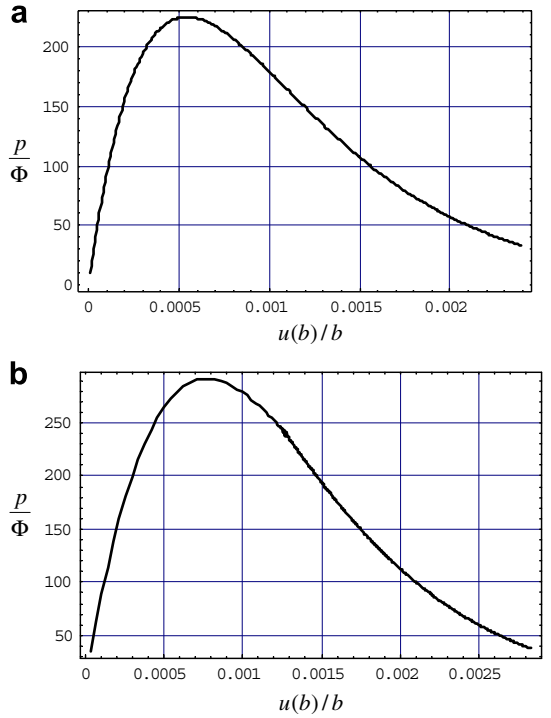

Fig. 4. Normalized pressure versus normalized displacement for spherical (a) and cylindrical (b) voids.

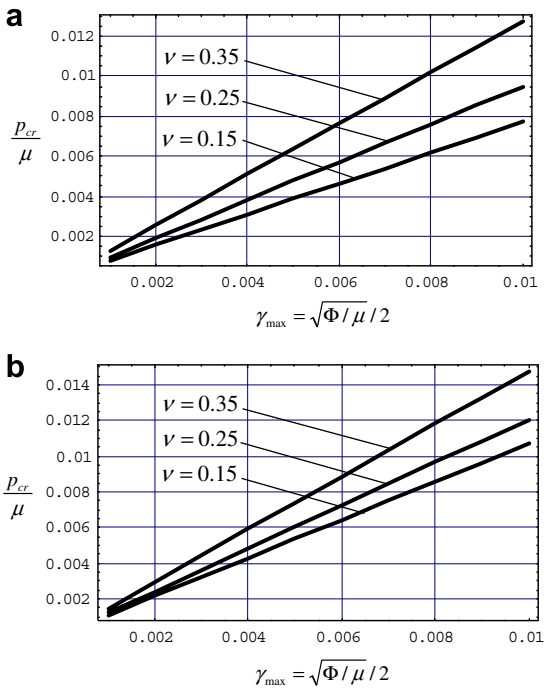

Fig. 5. Normalized critical tension versus normalized volumetric failure work for spherical (a) and cylindrical (b) voids with various Poisson ratios.

iteratively unless the normal stress at the outer surface $r = b$ converges to the given magnitude p and conditions $(2.25)_2$ or $(2.33)_2$ are obeyed.

Typical pressure–displacement curves are presented in Fig. 4 for spherical (a) and cylindrical (b) voids with $\mu/\Phi = 2.5 \times 10^5$ given in (2.8) and $K/\Phi = 3.75 \times 10^5$ given in (2.12). These curves do not change for $a/b < 0.01$, i.e. the critical tension is independent of the void size!

Fig. 5 presents parametric studies of the normalized critical tension p_{cr}/μ for different values of maximum shear strain γ_{max} and Poisson ratio ν, which are related to the normalized volumetric failure work and bulk modulus as follows: $\Phi/\mu = 4\gamma_{max}^2$ and $K/\mu = 2(1+\nu)/3(1-2\nu)$. The critical tension increases with the increasing work of material failure Φ as expected.

3. Griffith energy approach

Griffith (1921) energy approach consists of two steps. First, the solution of linear elasticity is obtained. Second, the energy balance is considered to provide creation of a new surface at the void edge.

3.1. Analysis of the spherical void expansion

In the case of linear elasticity, the setting of Section 2.2 is simplified with account of constant bulk and shear moduli. Particularly, (2.23) takes form

$$\begin{cases} \sigma_{rr} = 2\mu\varepsilon_{rr} + (K - 2\mu/3)\,\mathrm{tr}\,\boldsymbol{\varepsilon}, \\ \sigma_{\theta\theta} = 2\mu\varepsilon_{\theta\theta} + (K - 2\mu/3)\,\mathrm{tr}\,\boldsymbol{\varepsilon}, \\ \sigma_{\varphi\varphi} = 2\mu\varepsilon_{\varphi\varphi} + (K - 2\mu/3)\,\mathrm{tr}\,\boldsymbol{\varepsilon}. \end{cases} \tag{3.1}$$

Then equilibrium equation in terms of displacements reduces to the following form:

$$\frac{\partial^2 u}{\partial r^2} + 2\frac{\partial u}{r\partial r} - 2\frac{u}{r^2} = 0. \tag{3.2}$$

Its solution with account of boundary conditions (2.25) is

$$u = \frac{p}{1-(a/b)^3}\left(\frac{1-2\nu}{E}r + \frac{1+\nu}{E}\frac{a^3}{r^2}\right), \tag{3.3}$$

where elasticity modulus $E = 9K\mu/(3K+\mu)$ and Poisson ratio $\nu = (3K-2\mu)/2(3K+\mu)$ were used. Substituting this solution in kinematic (2.20) and constitutive (3.1) equations we have

$$\begin{cases} \varepsilon_{rr} = \frac{\partial u}{\partial r} = \frac{p}{1-(a/b)^3}\left(\frac{1-2\nu}{E} - \frac{2(1+\nu)}{E}\frac{a^3}{r^3}\right), \\ \varepsilon_{\theta\theta} = \frac{u}{r} = \frac{p}{1-(a/b)^3}\left(\frac{1-2\nu}{E} + \frac{1+\nu}{E}\frac{a^3}{r^3}\right), \\ \varepsilon_{\varphi\varphi} = \frac{u}{r} = \frac{p}{1-(a/b)^3}\left(\frac{1-2\nu}{E} + \frac{1+\nu}{E}\frac{a^3}{r^3}\right), \end{cases} \tag{3.4}$$

$$\begin{cases} \sigma_{rr} = \frac{p}{1-(a/b)^3}\left(1 - \frac{a^3}{r^3}\right), \\ \sigma_{\theta\theta} = \frac{p}{1-(a/b)^3}\left(1 + \frac{a^3}{2r^3}\right), \\ \sigma_{\varphi\varphi} = \frac{p}{1-(a/b)^3}\left(1 + \frac{a^3}{2r^3}\right). \end{cases} \tag{3.5}$$

Assuming $b \gg a$, we obtain the following strains and stresses at the void surface $r = a$:

$$\begin{cases} \varepsilon_{rr} = -(1+4\nu)p/E, \\ \varepsilon_{\theta\theta} = \varepsilon_{\varphi\varphi} = (2-\nu)p/E, \end{cases} \tag{3.6}$$

$$\begin{cases} \sigma_{rr} = 0, \\ \sigma_{\theta\theta} = \sigma_{\varphi\varphi} = 3p/2. \end{cases} \tag{3.7}$$

Let us consider, following Griffith, the energy balance during the void expansion. The total strain energy is

$$W_{\mathrm{T}} = \tfrac{1}{2}\left(4\pi b^2 p\right)u_b = 2\pi b^2 p u_b, \tag{3.8}$$

where $u_b \equiv u(r=b)$.

Suppose now that the void extends to radius $a+\delta a$ where δa is a small perturbation. In this case, new surface of area $4\pi(a+\delta a)^2 - 4\pi a^2 \cong 8\pi a\delta a$ is created. Thus, the energy release for the creation of this area can be written as follows

$$G8\pi a\delta a = 4\pi b^2 p\delta u_b - \delta W_{\mathrm{T}}, \tag{3.9}$$

where the first term on the right-hand side is for the work of the external forces and

$$u_b = u(b) = \frac{p}{1-(a/b)^3}\left(\frac{1-2\nu}{E}b + \frac{1+\nu}{E}\frac{a^3}{b^2}\right). \tag{3.10}$$

Substituting (3.10) in (3.9) we obtain

$$G8\pi a\delta a = 2\pi b^2 p\frac{\mathrm{d}u_b}{\mathrm{d}a}\delta a. \tag{3.11}$$

where

$$\frac{\mathrm{d}u_b}{\mathrm{d}a} = \frac{1-\nu}{E}\frac{6p(a/b)^2}{\left(1-(a/b)^3\right)^2}. \tag{3.12}$$

Thus, the energy release rate takes the form

$$G = \frac{3(1-\nu)}{2E}\frac{p^2 a}{\left(1-(a/b)^3\right)^2}, \tag{3.13}$$

If the critical energy release rate G_{c} is known for the given material, we can compute the critical tension for $b \gg a$:

$$p_{\mathrm{c}} = \sqrt{\frac{2EG_{\mathrm{c}}}{3(1-\nu)a}}. \tag{3.14}$$

Thus, the critical tension is inversely proportional to the square root of the void radius. The critical tension can increase unlimitedly with decrease of the radius.

3.2. Analysis of the cylindrical void expansion

In the case of linear elasticity, the setting of Section 2.3 is simplified with account of constant bulk and shear moduli. Particularly, (2.31) takes form

$$\begin{cases} \sigma_{rr} = 2\mu\varepsilon_{rr} + (K-2\mu/3)\,\mathrm{tr}\,\boldsymbol{\varepsilon}, \\ \sigma_{\theta\theta} = 2\mu\varepsilon_{\theta\theta} + (K-2\mu/3)\,\mathrm{tr}\,\boldsymbol{\varepsilon},, \\ \sigma_{zz} = (K-2\mu/3)\,\mathrm{tr}\,\boldsymbol{\varepsilon}. \end{cases} \tag{3.15}$$

Then equilibrium equation in terms of displacements reduces to the following form:

$$\frac{\partial^2 u}{\partial r^2} + \frac{\partial u}{r\partial r} - \frac{u}{r^2} = 0. \tag{3.16}$$

Its solution with account of boundary conditions (2.33) is

$$u = \frac{1+\nu}{E}\frac{p}{1-(a/b)^2}\left((1-2\nu)r + \frac{a^2}{r}\right). \tag{3.17}$$

Substituting this solution in kinematic (2.28) and constitutive (3.15) equations we have

$$\begin{cases} \varepsilon_{rr} = \frac{\partial u}{\partial r} = \frac{1+\nu}{E}\frac{p}{1-(a/b)^2}\left((1-2\nu) - \frac{a^2}{r^2}\right), \\ \varepsilon_{zz} = 0, \\ \varepsilon_{\theta\theta} = \frac{u}{r} = \frac{1+\nu}{E}\frac{p}{1-(a/b)^2}\left((1-2\nu) + \frac{a^2}{r^2}\right), \end{cases} \tag{3.18}$$

$$\begin{cases} \sigma_{rr} = \frac{p}{1-(a/b)^2}\left(1 - \frac{a^2}{r^2}\right), \\ \sigma_{\theta\theta} = \frac{p}{1-(a/b)^2}\left(1 + \frac{a^2}{r^2}\right), \\ \sigma_{zz} = \frac{2\nu p}{1-(a/b)^2}. \end{cases} \tag{3.19}$$

Assuming $b \gg a$ we obtain the following strains and stresses at the void surface $r = a$:

$$\begin{cases} \varepsilon_{rr} = -2\nu(1+\nu)p/E, \\ \varepsilon_{\theta\theta} = 2(1-\nu^2)p/E, \\ \varepsilon_{zz} = 0, \end{cases} \tag{3.20}$$

$$\begin{cases} \sigma_{rr} = 0, \\ \sigma_{\theta\theta} = 2p, \\ \sigma_{zz} = 2\nu p. \end{cases} \tag{3.21}$$

Let us consider, following Griffith, the energy balance during the void expansion. The total strain energy is

$$W_{\mathrm{T}} = \tfrac{1}{2}(2\pi b p)u_b = \pi b p u_b, \tag{3.22}$$

where $u_b \equiv u(r = b)$.

Suppose now that the void extends to radius $a + \delta a$ where δa is a small perturbation. In this case, new surface of area $2\pi(a+\delta a) - 2\pi a \cong 2\pi\delta a$ (for a unit height of the void) is created. Thus, the energy release for the creation of this area can be written as follows:

$$G 2\pi\delta a = 2\pi b p \delta u_b - \delta W_{\mathrm{T}}, \tag{3.23}$$

where the first term on the right-hand side is for the work of the external forces and

$$u_b = u(b) = \frac{1+\nu}{E}\frac{pb^2}{b^2 - a^2}\left((1-2\nu)b + \frac{a^2}{b}\right). \tag{3.24}$$

Substituting (3.24) in (3.23) we obtain

$$G 2\pi\delta a = \pi b p \frac{\mathrm{d}u_b}{\mathrm{d}a}\delta a. \tag{3.25}$$

where

$$\frac{\mathrm{d}u_b}{\mathrm{d}a} = \frac{1-\nu^2}{E}\frac{4pb^3 a}{(b^2 - a^2)^2}. \tag{3.26}$$

Thus, the energy release rate takes the form

$$G = \frac{1-\nu^2}{E}\frac{2p^2 b^4 a}{(b^2 - a^2)^2}, \tag{3.27}$$

If the critical energy release rate G_{c} is known for the given material, we can compute the critical tension for $b \gg a$:

$$p_{\mathrm{c}} = \sqrt{\frac{E G_{\mathrm{c}}}{2(1-\nu^2)a}}. \tag{3.28}$$

Again, like in the previous section the critical tension is inversely proportional to the square root of the void radius. The critical tension can increase unlimitedly with decrease of the radius.

4. Discussion

A constitutive theory of softening hyperelasticity for modeling failure of isotropic solids has been developed and applied to the problem of cavitation. The exponential stored energy expression describes material failure via strain softening. The material bulk modulus and the shear modulus of an isotropic material are completed with a new constant—the volumetric failure work, which controls softening. The material model is interpreted based on the simple shear and hydrostatic pressure examples. The distortional (deviatoric) deformation at the given point exhibits behavior analogous to the simple shear, which graph is shown in Fig. 2a. The dilatational (volumetric) deformation at the given point exhibits behavior analogous to the hydrostatic pressure, which graph is shown in Fig. 2b. The softening hyperelasticity framework is applied to the problem of spherical and cylindrical void growth under hydrostatic tension. The force–displacement curves are tracked numerically (Fig. 4) and the critical tension is calculated. It is found that the critical tension does not depend on the size of the void for small voids. This result is intuitively expected because the constitutive model does not include the characteristic length. Parametric studies of the dependence of the critical tension on the parameter of the volumetric failure work are performed. It is shown that the critical tension increases with the increase of the magnitude of the volumetric failure work (Fig. 5).

Besides, an alternative analysis of cavitation is considered based on the Griffith energy approach. It is found that the critical tension depends on the size of the void—Eqs. (3.14) and (3.28). The latter notion leads to a controversial conclusion that the critical tension can increase unlimitedly with the decrease of the void size. It is important to realize that controversial results of the Griffith approach are not inherent in the problems of the spherical or cylindrical void growth only. There is a general issue of size dependence concerning the Griffith approach. To illustrate this point, let us consider an elliptic cavity/crack. We assume that the cavity is small as compared to the size of the hosting body. In this case, the stress/strain concentration at the edge of the cavity is independent of the cavity size though it depends on the ratio of the elliptic radii. Even in the limit case of an ideal mathematical crack when the ratio of the elliptic radii approaches zero and the stress state is singular, there is no size dependence in stresses and strains. The size independence of the solution of cavity problem is a consequence of the fact that the elasticity theory and the classical continuum mechanics are length-independent. Contrary to these theories, the Griffith approach is length-dependent because it introduces the surface energy in analysis and the G/E ratio, for example, sets up the characteristic length. Introduction of the characteristic length in the Griffith approach is not in peace with the basic formulation of the classical continuum mechanics. Evidently, the Griffith criticality condition is separated from stress analysis both physically and mathematically. We find this fact discouraging and emphasize the necessity to include the criticality (failure) conditions directly in the constitutive model of materials.

It should not be missed, however, that the discussed above independence of the solution on the defect size is violated in the following two limit cases. The first limit case corresponds to a defect whose size is comparable with the size of the hosting structure. It is not a simple matter to define the comparability; actually, the stress/strain state in a structure under consideration will affect such a definition. It is important, however, that in this case the continuum mechanics analysis will 'feel' the size of the defect. The latter means, particularly, that the critical tension for a big spherical cavity in the softening hyperelasticity analysis considered in our work will depend on the ratio between the cavity size and the hosting sphere radius. In other words, the classical continuum mechanics with the embedded material failure conditions will exhibit the length-dependence for a big defect. Another limit case is a very small cavity. The classical continuum mechanics may not be applicable at very small length scales and an enhanced continuum formulations can be required where the characteristic lengths are a part of the general theoretical framework like in the case of strain-gradient plasticity (Hutchinson, 2000), for instance. We believe, however, that the generalized continuum formulation should include a possible mechanism of the material failure as its integral part and not as a separate condition like in the case of the Griffith approach.

Concerning the cavitation problem considered in the present work it should be noted that a number of approaches based on various nonlinear elasticity theories, including those called 'deformation plasticity', have

been considered in the literature: Bassani et al. (1980), Ball (1982), Abeyaratne and Horgan (1985), Huang et al. (1991), Fond (2001). Cavitation instabilities were described in these works based on various constitutive models. It is interesting, however, that none of these models included strain softening on purpose as it is done in the present work where the softening is controlled by a material constant, ϕ.

Considering restrictions of the present study we should emphasize that the softening hyperelasticity approach was used in the above calculations for the prediction of the critical state of deformation where the onset of global instability occurs due to material failure. When the general postcritical evolution of failure is of interest two numerical problems concerning the finite element implementation of softening hyperelasticity should be addressed. First, it is necessary to introduce the energy dissipation in the finite element model in order to preclude from the material healing. This can be done, for example, by decreasing the material constants within a finite element by few orders of magnitude after the element energy reaches the critical value of the volumetric failure work. In other words, the damaged material should have new and low magnitudes of the material constants. The second issue is related with the necessity to regularize the ill-posed numerical problem where the loss of ellipticity/hyperbolicity of the governing equations with softening can lead to the pathological mesh-sensitivity[1] (Crisfield, 1997; Belytschko et al., 2000; de Borst, 2001). The regularization procedure should introduce a characteristic length in the calculation precluding the mesh sensitivity. Three following approaches are considered in the literature to regularize the numerical problem of the FE-mesh sensitivity. The first approach suggests replacing the classical continuum formulation with a generalized continuum formulation—higher-order, gradient, or non-local theories (de Borst and van der Giessen, 1998). The generalized continuum formulations introduce material length parameters, which control the strain localization processes. The only shortcoming of the generalized continuum formulations is the need to give a clear physical interpretation to the necessary additional boundary conditions. The second approach goes back to the work of Hillerborg et al. (1976). The basic idea of this approach is to introduce a characteristic material length directly in the FE model bypassing the PDE formulation. This approach proved itself in numerical simulations suppressing the pathological mesh sensitivity and it was adapted by ABAQUS for analysis of concrete structures. The third approach to the treatment of mesh sensitivity can be called dynamic regularization. The basic idea of this approach is to introduce the characteristic length in the problem implicitly through the rate dependence of the constitutive or balance equations. Needleman (1988), for example, observed that rate-dependence of the material regularizes the ill-posed numerical problem. He notes, however, that whether or not the introduced implicit length-scale is relevant depends on the particular circumstances. Another sort of regularization was reported by Zhang et al. (2002), who added the viscous forces to the momentum balance equations within the framework of the VIB method. They observed in simulations that the artificial dumping suppressed the mesh sensitivity. These results are promising and they can be applied for the regularization of the failure evolution problem within the framework of the softening hyperelasticity theory proposed in the present work.

References

Abeyaratne, R., Horgan, C.O., 1985. Initiation of localized plane deformations at a circular cavity in an infinite compressible nonlinearly elastic medium. Journal of Elasticity 15, 243–256.

Ball, J.M., 1982. Discontinuous equilibrium solutions and cavitation in nonlinear elasticity. Philosophical Transactions of the Royal Society of London. Series A – Mathematical Physical and Engineering Sciences 306, 557–611.

Bassani, J.L., Durban, D., Hutchinson, J.W., 1980. Bifurcation of a spherical hole in an infinite elastoplastic medium. Mathematical Proceedings of the Cambridge Philosophical Society 87, 339–356.

Bazant, Z.P., Planas, J., 1998. Fracture and Size Effect of Concrete and Other Quasibrittle Materials. CRC Press, Boca Raton.

Belytschko, T., Liu, W.K., Moran, B., 2000. Nonlinear Finite Elements for Continua and Structures. Wiley, New York.

Broberg, K.B., 1999. Cracks and fracture. Academic Press, London.

Crisfield, M.A., 1997. Non-linear Finite Element Analysis of Solids and Structures, vol. 2. Wiley, Chichester.

de Borst, R., 2001. Some recent issues in computational failure mechanics. International Journal for Numerical Methods in Engineering 52, 63–95.

de Borst, R., van der Giessen, E., 1998. Material Instabilities in Solids. Wiley, Chichister.

[1] The postcritical calculations of cavitation in the present work were numerically stable because mesh sensitive modes of deformation were filtered out by the symmetry assumption.

Fond, C., 2001. Cavitation criterion for rubber materials: A review of void-growth models. Journal of Polymer Science: Part B: Polymer Physics 39, 2081–2096.
Gao, H., Klein, P., 1998. Numerical simulation of crack growth in an isotropic solid with randomized internal cohesive bonds. Journal of the Mechanics and Physics of Solids 46, 187–218.
Gao, H., Ji, B., Jager, I.L., Arzt, E., Fratzl, P., 2003. Materials become insensitive to flaws at nanoscale: Lessons from nature. Proceedings of the National Academy of Sciences 100, 5597–5600.
Griffith, A.A., 1921. The phenomena of rupture and flow in solids. Philosophical Transactions of the Royal Society of London, Series A 221, 163–198.
Hertzberg, R.W., 1989. Deformation and Fracture of Engineering Materials. Third ed.. Wiley.
Hillerborg, A., Modeer, M., Peterson, P.E., 1976. Analysis of crack growth in concrete by means of fracture mechanics and finite elements. Cement and Concrete Research 6, 773–782.
Huang, Y., Hutchinson, J.W., Tvergaard, V., 1991. Cavitation instabilities in elastic–plastic solids. Journal of the Mechanics and Physics of Solids 39, 223–241.
Hutchinson, J.W., 2000. Plasticity at the micron scale. International Journal of Solids and Structures 37, 225–238.
Ji, B., Gao, H., 2004. A study of fracture mechanisms in biological nano-composites via the virtual internal bond model. Materials Science and Engineering A366, 96–103.
Kachanov, L.M., 1958. Time of the rupture process under creep conditions. Izvestiia Akademii Nauk SSSR, Otdelenie Teckhnicheskikh Nauk 8, 26-31.
Kachanov, L.M., 1986. Introduction to Continuum Damage Mechanics. Martinus Nijhoff Dotrecht, Netherlands.
Kanninen, M.F., Popelaar, C., 1973. Fundamentals of Fracture Mechanics. Butterworth, London.
Klein, P., Gao, H., 1998. Crack nucleation and growth as strain localization in a virtual-bond continuum. Engineering Fracture Mechanics 61, 21–48.
Knott, J.F., 1985. Advanced Fracture Mechanics. Oxford University Press.
Krajcinovic, D., 1996. Damage Mechanics. North Holland Series in Applied Mathematics and Mechanics. Elsevier.
Lemaitre, J., Desmorat, R., 2005. Engineering Damage Mechanics: Ductile, Creep, Fatigue and Brittle Failures. Springer, Berlin.
Needleman, A., 1988. Material rate dependence and mesh sensitivity in localization problems. Computer Methods in Applied Mechanics and Engineering 67, 69–85.
Skrzypek, J., Ganczarski, A., 1999. Modeling of Material Damage and Failure of Structures. Springer, Berlin.
Volokh, K.Y., 2004. Nonlinear elasticity for modeling fracture of isotropic brittle solids. Journal of Applied Mechanics 71, 141–143.
Volokh, K.Y., Gao, H., 2005. On the modified virtual internal bond method. Journal of Applied Mechanics 72, 969–971.
Volokh, K.Y., Ramesh, K.T., 2006. An approach to multi-body interactions in a continuum-atomistic context: application to analysis of tension instability in carbon nanotubes. International Journal of Solids and Structures 43, 7609–7627.
Zhang, P., Klein, P., Huang, Y., Gao, H., Wu, P.D., 2002. Numerical simulation of cohesive fracture by the virtual-internal-bond method. Computer Modeling in Engineering and Sciences 3, 263–277.
Zhang, P., Jiang, H., Huang, Y., Geubelle, P.H., Hwang, K.C., 2004. An atomistic-based continuum theory for carbon nanotubes: analysis of fracture nucleation. Journal of the Mechanics and Physics of Solids 52, 977–998.